High Power X-Ray Point Source For Next Generation Lithography

I.C.E. Turcu, R. Forber, R. Grygier, H. Rieger, M. Powers, S. Campeau, G. French, R. Foster, P. Mitchell, C. Gaeta, Z. Cheng[a], J. Burdett[a], D. Gibson[a], S. Lane[b], T. Barbee[b], S. Mrowka[c], J.R. Maldonado[d]

JMAR Technologies, Inc., 3956 Sorrento Valley Blvd., San Diego, CA 92121.
[a] X-ray Optical Systems, Inc., 90 Fuller Rd, Albany, NY 12205.
[b] Lawrence Livermore National Laboratory, 7000 East Avenue, P.O. Box 808, L 399, CA 94551.
[c] Oxford Research Group, 119 Cynthia Drive, Pleasant Hill CA 94523.
[d] ETEC Systems, 26460 Corporate Avenue, Hayward, CA 94545.

Key words: X-ray source, X-ray Lithography, Diode Pumped Laser, Laser-Plasma.

ABSTRACT

An x-ray power of 2.8 Watts at the 1 nm x-ray lithography wavelength was generated by a copper plasma formed by a single laser beam focused to an intensity of $>10^{14}$ W/cm^2 on a copper tape target. The all solid state Britelight™ YAG laser has 700 ps pulse duration, 300 Hz pulse repetition rate, average power of 75 Watts, and < 2 times diffraction limited beam quality at the fundamental 1.064 μm wavelength. The single beam laser system has a master oscillator, a preamplifier and one power amplifier, all diode pumped. Measurements confirmed negligible copper vapor debris at 8 cm from the laser-plasma source with atmospheric pressure He gas and modest gas flow. The point source x-ray radiation was collimated with either a polycapillary or grazing mirror collimator. The near-parallel beam of x-rays has good divergence both globally (0.5mrad) and locally (<3 mrad), good uniformity (2% achievable goal) and large uniform field size (20 mm x 20 mm full field and 25mm x 36mm scanning system). High-resolution lithography was performed for the first time with collimated 1 nm point source x-rays. A power scaling system is being built with eight amplified beams in parallel on the x-ray target, and is expected to achieve 24-30 Watts of x-rays. A 16 beam laser plasma x-ray lithography system could achieve a throughput of 24 wafer levels per hour using 300 mm diameter wafers.

1. INTRODUCTION

X-ray lithography (XRL) is a leading contender for Next Generation Lithography (NGL) tools capable of printing 100 nm size features and smaller for future semiconductor memories and processors as well as magnetic heads. While XRL technology has been fully demonstrated, two key issues require more work. The first is the 1-to-1 proximity x-ray mask with sub-100 nm features, which is being addressed both in the US and Japan. The second issue is the availability of a compact x-ray source. Presently, Synchrotron Radiation Sources (SRS) (e.g. Oxford Instruments, UK) are used for x-ray lithography. The synchrotron capital cost is high, but one synchrotron can feed 6-12 steppers. There has been a reluctance to adopt XRL, however, because of the high initial cost and the time required to modify current factory designs to accommodate SRS. Hence, there is a need for a compact x-ray source at 1nm wavelength for single stepper use, that is low cost and sized no larger than today's optical lithography stations, for process development, and for low and high volume manufacturing[1].

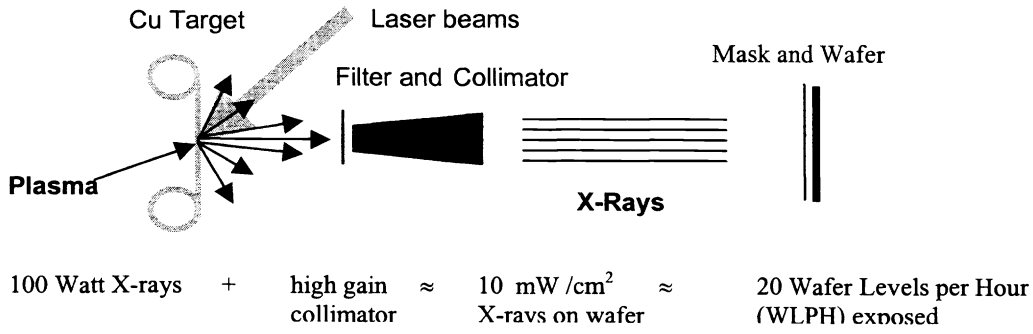

Fig. 1. Compact laser-plasma x-ray source for lithography. A 20 Wafer Level per Hour lithographic capability requires 100 Watts of x-ray power radiated by the plasma source, a high gain collimator, and a sensitive photoresist.

Part of the SPIE Conference on EUV, X-Ray, and Neutron Optics and Sources
Denver, Colorado • July 1999
SPIE Vol. 3767 • 0277-786X/99/$10.00

JMAR is developing such a compact Picosecond X-ray Source (PXS), under a DARPA contract. In the JMAR x-ray source the radiation is generated by a high temperature copper plasma heated by high intensity laser pulses focused on the copper target. The paper describes: the all solid state laser system which can deliver high intensity pulses on target at high laser average power; the high power source of x-rays which also has negligible wafer contamination from target debris; x-ray collimator optics which turns the diverging plasma radiation into a parallel x-ray beam required for proximity lithography; 200nm structures printed on silicon wafers from an x-ray mask using the 1nm x-ray beam; scaling of the x-ray power of the PXS. Figure 1 shows the schematic of a x-ray lithography system using a laser-plasma x-ray source with collimated radiation. High throughput lithography of around 20 wafer levels per hour require approximately 100 Watt of x-ray power emitted by the source as well as the efficient x-ray collection by the collimator. Figure 2 shows JMAR's Picosecond X-ray Source (PXS) concept for high power x-ray generation. The laser amplifier modules amplify the laser pulses from the master oscillator and pre-amplifier. The infrared laser pulses are converted to green. Green laser beams can be focused in the x-ray chamber in He gas at atmospheric pressure at high x-ray conversion efficiency with minimal target debris. The laser beams are combined and focused on the copper target to form a distribution of plasma x-ray sources. The diverging radiation is collected and turned into a parallel x-ray beam by the collimator.

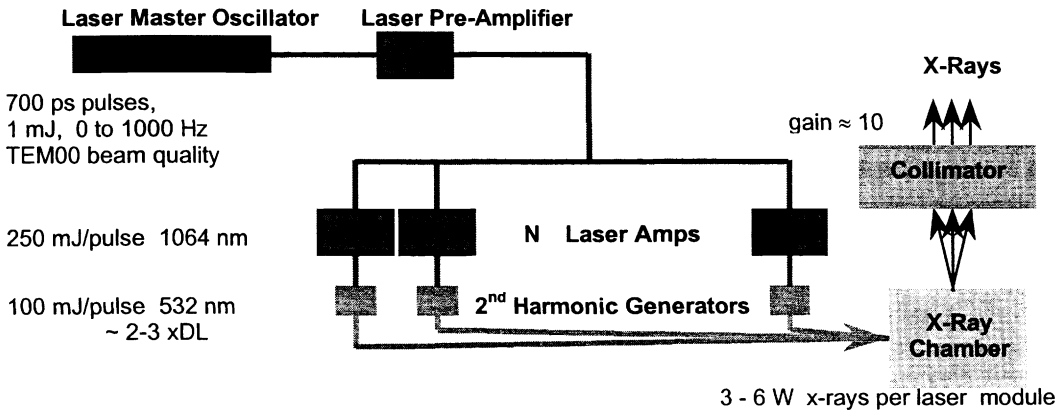

Fig. 2. JMAR's Picosecond X-ray Source (PXS) concept for high power x-ray generation. The laser amplifier modules amplify the laser pulses from the master oscillator and pre-amplifier. The infrared laser pulses are converted to green. Green laser beams can be focused in the x-ray chamber in He gas at atmospheric pressure and increase the laser to x-ray conversion efficiency. The laser beams are combined and focused on the copper target to form a distribution of plasma x-ray sources. The diverging radiation is collected and turned into a parallel x-ray beam by the collimator.

2. 75 WATT DIODE PUMPED SOLID STATE LASER AMPLIFIER MODULE

JMAR has developed a compact high power diode pumped all solid state laser [2], Britelight™ for x-ray generation. The complete system contains eight to sixteen laser amplifier modules as shown in Fig. 2. To test the system we performed x-ray generation using one laser master oscillator, a laser pre-amplifier stage, and one laser amplifier module.

Figure 3a shows a schematic of the laser master oscillator and laser amplifier module. The laser pre-amplifier is similar to the laser amplifier except that it has only one diode pumped Nd:YAG rod. The laser oscillator operates Q-switched, mode-locked, and cavity dumped. This results in short laser pulses of 150 ps – 2000 ps duration, with high energy per pulse of ~1 mJ, very good beam quality of 1.2 x diffraction limit, and high repetition rate of up to 1000 Hz. The fundamental laser wavelength is 1064 nm. The development laser oscillator has a demonstrated lifetime of more than one billion laser pulses. The development laser oscillator used in the present x-ray experiments is shown in Fig. 4a in the box at right, which also includes a laser pre-amplifier stage. A commercial version of the laser oscillator is available in JMAR's Britelight™ laser family, entitled the BL-1001 laser. Figure 4b shows the prototype BL-1001 laser in its black anodized box ready for tuning, on the left side of the figure.

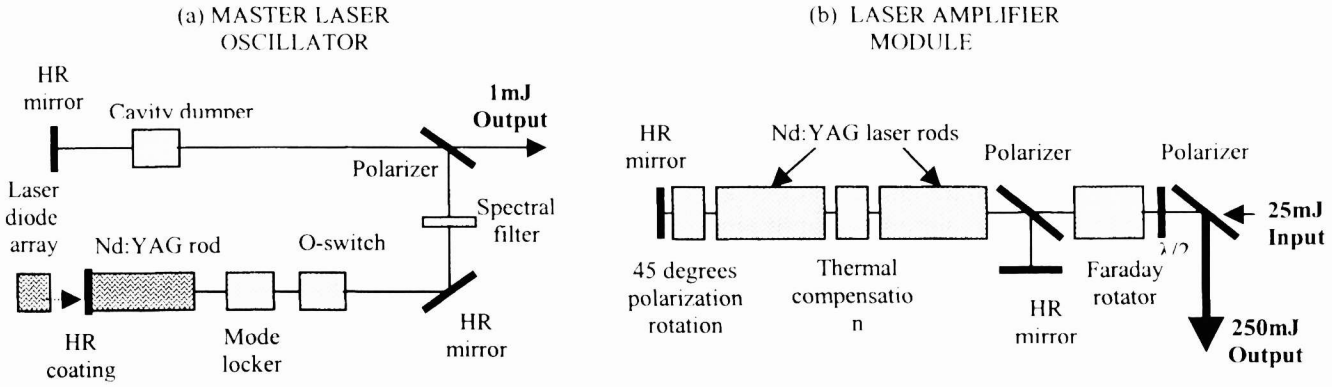

Fig. 3 Schematic of the diode pumped picosecond laser: (a) master oscillator, and (b) diode pumped 4 pass laser amplifier module.

The laser preamplifier has one transverse pumped Nd:YAG rod and operates in four pass amplification similar to the amplifier shown in Fig. 3b. The laser preamplifier has an output of 700ps pulse duration, 25 mJ pulse energy, 0-500 Hz repetition rate (1 kHz under development) with 1.4 x diffraction limit beam quality. Figure 3b shows the four-pass amplifier with two diode pumped Nd:YAG laser rods. The laser amplifier retains the 700 ps pulse duration, and has 250 mJ pulse energy. It has achieved 0-300 Hz repetition rate (1 kHz under development) with ~2x diffraction limit beam quality. Figure 4c shows the fluorescence emission from the laser rod when pumped by laser diodes. It is expected that implementing the improved pumped uniformity shown at the right of Fig. 4c can increase the repetition rate and average laser power emitted by the laser amplifier. Figure 4a shows the development laser amplifier (in the box at left) and Fig. 4b shows the prototype-engineered version (on the right). The footprint of the development 75 Watt laser system shown in Fig. 4a is 4ft x 3ft x 1ft.

The extremely high beam quality and peak and average laser power as well as the small footprint of the laser system are all due to the very efficient laser diode pumping process. The wall plug efficiency of the laser diodes is 50% and the overall wall plug efficiency of the laser system is >10%. This excellent power efficiency is the key advantage for using such a laser system for high power x-ray generation.

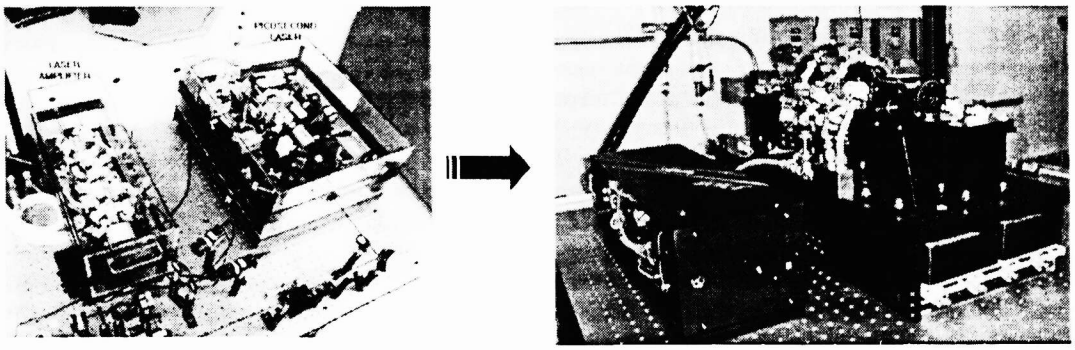

(a) Development 75 W laser system

(b) Prototype Laser Master Oscillator and Amplifier

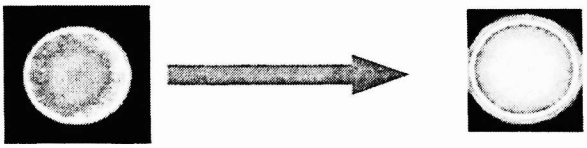

(c) Fluorescence emission from diode-pumped laser rod

Present laser diode pump uniformity

Improved laser diode pump uniformity

Fig. 4. Diode pumped, all solid state Britelight™ lasers. (a) Development 75 W laser system. Laser oscillator and pre-amplifier on the right and two head power amplifier on the left. (b) BL-1001 commercial laser master oscillator (left) and brassboard amplifier (right). (c) Fluorescence emission from diode-pumped laser rod. The improved pump uniformity is expected to lead to increased repetition rate and higher average amplifier power.

3. PLASMA X-RAY SOURCE GENERATING 2.8 WATTS OF 1NM RADIATION

When the Britelight™ laser is focused on the copper tape target it generates a very hot copper plasma which radiates an intense x-ray flux. The maximum infrared laser intensity on target is 9 x 10^{14} W/cm^2. This corresponds to a laser pulse of 250 mJ energy, 700 ps duration and focused to a 7 μm spot diameter on target. Such high laser intensity on target will heat up the copper plasma to a temperature of a few million degrees Kelvin. At this temperature the plasma is highly ionized containing mainly Cu XXI ions which emit Cu L-shell x-rays. The emission is also called neon-like because the Cu ions have only ten electrons left, just like the Ne atom, and therefore will emit the neon spectrum shifted to 1nm wavelength. The Cu L-shell emission x-ray spectrum is centered at 1nm wavelength and extends from 0.8nm to 1.2nm[1, 3]. At such high plasma temperatures a high density (near solid density) copper plasma will efficiently convert the focused laser energy into 1nm x-ray energy.

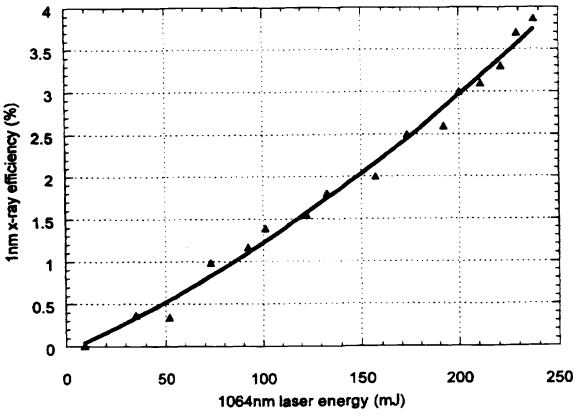

Fig. 5 Laser to x-ray energy conversion efficiency as a function of laser pulse energy. The 1 nm x-rays are emitted by the hot copper plasma formed when the laser is focused on the copper tape target.

The IR (λ= 1064nm) laser to 1 nm x-ray conversion efficiency is shown in Fig. 5 as a function of the laser pulse energy. A high x-ray conversion efficiency of 4% is reached at the maximum laser intensity of 9 x 10^{14} W/cm^2, which corresponds to 250 mJ laser pulse energy. The conversion efficiency increases monotonically for the laser energy range covered. It is therefore expected that it will increase to the maximum reported[4] efficiency of 7% if the laser energy on target is increased. For example, this could be achieved by superimposing two laser pulses of 250 mJ each, the two laser beams coming from two of the parallel amplifiers of Fig. 2. When the laser beam energy is converted from infrared (λ = 1064nm) to green (λ = 532 nm) the maximum x-ray conversion efficiency measured is 6%. The gain in x-ray conversion efficiency is offset by the efficiency of converting infrared laser radiation to green. Nevertheless, there are two factors which weigh heavily in favor of green conversion of laser radiation. One is the even higher maximum x-ray efficiency, which could be obtained by superimposing two green laser pulses, as discussed above in the case of two IR laser pulses. The second reason is the preferred operation of the x-ray chamber filled with atmospheric pressure He gas, as will be discussed in the next section. This is not possible when focusing an IR laser beam into the x-ray chamber because of laser breakdown in the He gas at a pressure higher than 100 torr.

In order to increase the x-ray average power emitted by laser plasma source, the repetition rate of the laser is increased from 120 Hz to 300 Hz. Table 1 shows the measured x-ray source average power at 1nm wavelength radiated at increasing laser repetition rate. The emitted x-ray energy per laser pulse is measured with a Quantrad P-I-N silicon x-ray diode is coated with 0.5 μm Al film and is filtered with 4.0 μm of Aluminum foil. The x-ray diode was cross-calibrated for x-ray lithography applications against a standard based on x-ray exposure of photoresist with 1nm radiation. The x-ray power emitted increases linearly with the laser rep rate and average power. The average x-ray energy emitted for each laser pulse is multiplied with the laser repetition rate to obtain the x-ray average power emitted by the plasma source. A record 1nm x-ray average power of 2.8 Watt is obtained for a laser power of 75 Watt at a laser pulse repetition rate of 300 Hz. The x-ray conversion efficiency is constant at around 4% when the laser repetition rate is increased from 100Hz up to 300 Hz. This confirms that the laser beam quality is maintained at high repetition rates and high laser average powers. The laser beam quality of the present laser amplifier degrades slightly at 400 Hz such that it is not yet useful for x-ray generation. Nevertheless, it is

expected that the x-ray average power will continue to scale linearly with the repetition rate when the upgraded, laser amplifier (with improved pump uniformity as discussed in Section 2) is introduced in the system.

Table 1. X-ray source average power at 1nm wavelength radiated at increasing laser repetition rate.

Laser repetition rate [Hz]	IR laser energy per pulse [mJ]	IR laser average power [W]	1nm x-ray average power [W] in 2π sr.	Laser to x-ray conversion efficiency [%]	Optical system transmission [%]
120	**238**	**28.6**	**1.1**	**3.9%**	**98%**
200	**235**	**47.0**	**1.8**	**4.1%**	**95%**
300	**250**	**75.0**	**2.8**	**3.9%**	**98%**
400	**223**	**89.2**	**TBD**		

4. PLASMA X-RAY SOURCE WITH NEGLIGIBLE TARGET DEBRIS

A hot and dense plasma source is a very bright source of soft x-ray but at the same time a potential source of target material deposition. When the plasma is used as a radiation source, the x-ray chamber and x-ray beamlines need to be free of contamination with target material. The target debris is generated due to the very high temperature (millions of degrees K) and high density (solid density) copper plasma. The product of temperature and density results in a very large pressure of hundreds of millions of atmospheres generated in the plasma. This extreme state of matter is established in a very small volume of 7μm diameter at the laser focus and has very short time duration of 700 ps. Nevertheless copper ions are ablated from the target at very high speeds (typically[1] ~10^7 cm/s) and a strong shock is sent into the target material. Several methods can be used to reduce and eliminate the x-ray chamber contamination with target material, when a solid target is used[1]:

(a) Use a very thin tape target (copper for 1 nm x-rays). The plasma-generated shock wave breaks through the tape and ejects the target material at the back of the target where it can be collected. If thick solid target material is used, the shock wave is reflected back to the target surface and splashes the x-ray chamber with target droplets;

(b) Fill the chamber with He gas. The gas stops the ablated Cu ions. The stopping power for the Cu ions is enhanced by the fact that the He gas is ionized by the intense plasma radiation;

(c) Flow He gas across the volume in which the Cu ions are stopped to remove the target material from the x-ray chamber.

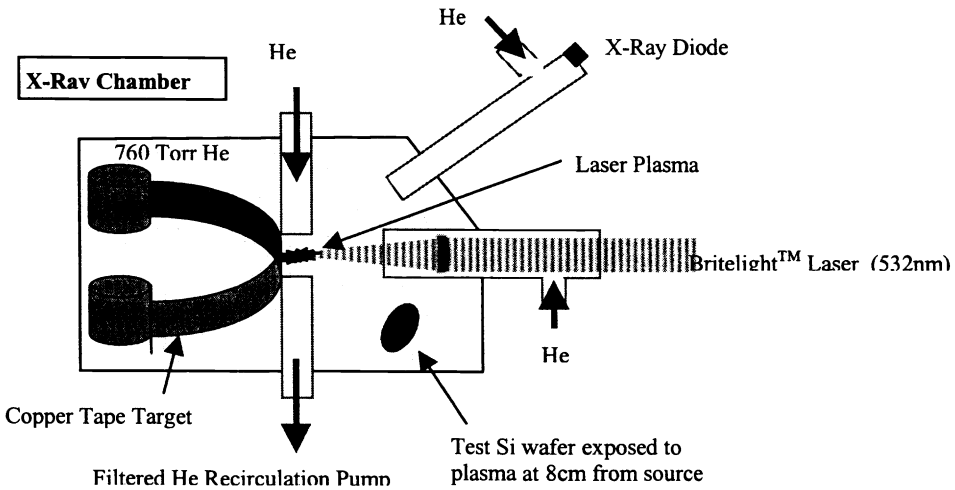

Fig. 6. X-ray source emitting 1nm radiation from a high temperature copper plasma generated by the high intensity Britelight™ laser. The x-ray chamber is filled with He gas at 1 atm. and the laser radiation is converted from IR to green. He gas stops the Cu plasma ions and helium flow (in central tube) purges and filters the Cu atoms from the chamber. A positive He pressure is maintained at the focusing lens, test wafer and x-ray detector.

JMAR has developed a negligible contamination x-ray chamber shown schematically in Fig. 6. The x-ray chamber is filled with He gas at atmospheric pressure and the laser radiation is converted from IR to green. A green laser beam can be focused without causing breakdown in the helium gas at atmospheric pressure; this breakdown inhibits coupling energy to the copper. When an infrared laser beam is used the He pressure in the x-ray chamber needs to be lowered to 80 Torr to avoid

gas breakdown. He gas stops the Cu plasma ions and a laminar helium flow (in the central tube) purges and filters the copper atoms from the chamber. The 300 liter•atm per min He flow in the central tube is generated by a re-circulation pump. The He gas is filtered by a HEPA filter before being returned to the x-ray chamber. A positive He pressure is maintained at the focusing lens, test wafer and x-ray detector by a smaller He flow of 27 liter•atm per min, as shown in Fig. 5.

The copper target debris deposition is measured on the test wafer placed in the x-ray chamber as shown in Fig. 6, at a distance of 8 cm from the plasma at the position where a collimator is placed (see Section 5). The wafer is exposed to the plasma radiation and material emerging from the plasma at an angle of 25° with respect to the normal to the target. The 5" diameter wafer is held in a metal box with an opening such that an area of slightly larger than 1" diameter was directly exposed to the plasma. The wafer can be rotated such that several exposures can be carried out on the same wafer. A positive He pressure is kept in the wafer holder by He feed pipes.

Three wafer exposures were carried out. Each exposure was one hour long or one million laser shots on the copper tape target. The laser repetition rate was 300Hz. The wafer exposures were delivered at three different He pressures in the x-ray chamber: 70 Torr (IR laser), 150 Torr (green laser) and 760 Torr (green laser). After exposure the wafers were sent for contamination analysis to the IBM Hopewell Junction Analytical Services Facility. The copper contamination of the wafers was measured by Total Reflection X-Ray Fluorescence (TXRF). The error bars on the contamination measurements was less than ± 15% for a few times 10^{10} atoms/cm^2. The number of copper atoms deposited by the plasma was obtained by subtracting the number of Cu atoms measured in the unexposed area (background) from the number measured in the exposed area (signal). The background measured on the wafer kept at 760 torr He was comparable to that of a virgin wafer. For the wafer kept at 150 torr and 70 torr He, the background was higher but still a factor of 1200 and 14 times respectively, smaller than the Cu signal. The higher background signal shows that at low pressures (70 Torr and 150 Torr) in the x-ray chamber there still is some copper diffusion in He gas in the x-ray chamber. If the lithographic system is required to run at low He pressure, sealing the x-ray window of the collimator housing (see Fig. 1) eliminates the diffused He atoms from the collimator and x-ray beamline (Section 5).

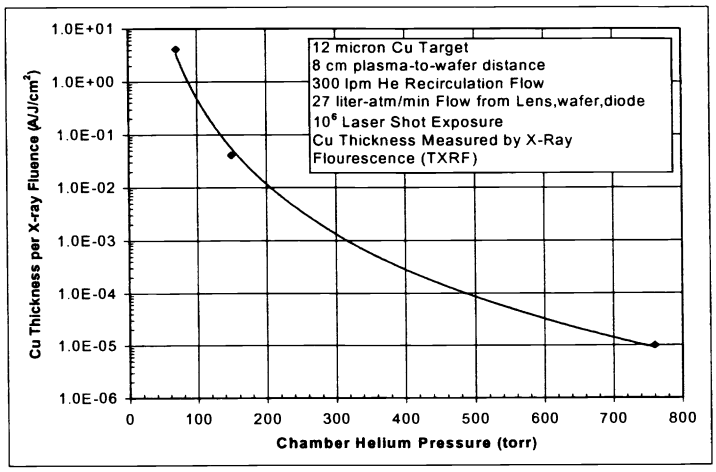

Fig. 7. Copper target debris accumulation for 10^6 laser shots as a function of helium gas pressure in the x-ray chamber. The Angstrom thickness of the copper film deposited on the wafer is normalized to the x-ray fluence (in J/cm^2) at the wafer placed 8 cm from the plasma source at an angle of 25° from the target normal. See text.

The Copper target material accumulation on the test wafer is plotted in Fig. 7 as a function of helium gas pressure in the x-ray chamber. The thickness (in Angstroms) of the copper film deposited on the wafer is normalized to the x-ray fluence (in J/cm^2) at the wafer. Two main conclusions can be drawn from Fig. 7:

1. Negligible Cu deposition is observed when the wafer was exposed for one million laser-plasma pulses at atmospheric pressure helium with the flow system shown in Fig. 6. The measured copper thickness normalized to the x-ray fluence at the wafer is 10-5 Å/(J/cm2). We can now estimate the time it takes to coat the collimator (Fig. 1) x-ray window with a copper layer which absorbs 1% of the x-rays. This appears to be a good indication of the acceptable amount of target material contamination during the x-ray lithographic process. From the above-normalized copper thickness we calculate that it would take 530 hours of the full power lithographic x-ray source (>100 W x-ray power) operation to reduce the transmission of the collimator x-ray window by 1%. This is for an x-ray power of 20 mW /cm2 delivered at the photo-resist by the system in Fig. 1 with the x-ray chamber filled with

atmospheric pressure helium which is flown as in Fig. 6. The x-ray window sealing the x-ray collimator from the x-ray chamber could be a thin Si3N4 membrane or a thin plastic filter as used in the present experiments.

2. The deposited copper thickness increases as the He pressure in the x-ray chamber decreases. The exposure time for 1% drop in x-ray window transmission in front of the collimator also decreases with decreasing helium pressure in the x-ray chamber. Compared to the above 530 hours at atmospheric He pressure, the exposure time would be 7.7 minutes at 150 torr and 4.6 seconds at 70 torr He pressure. Nevertheless, one could use a moving plastic film as the collimator x-ray filter and seal. The plastic film, 3 cm wide, would need to move at a modest speed of 0.7 cm/s to maintain its high x-ray transmission if the He pressure in the x-ray chamber is kept at 70 torr. This may arise if the IR laser beam is focused directly into the x-ray chamber rather than first converting it to green.

5. PARALLEL X-RAY BEAM FROM COLLIMATED PLASMA RADIATION

It is essential to have a parallel beam x-rays for proximity lithography at 100 nm, and below. The compact plasma source of x-rays is a point source emitting diverging radiation into the 2π steradians half space bounded by the x-ray target surface. The radiation angular distribution is smooth and symmetric with respect to the target normal. The x-ray emission follows1 a $(\text{cosine } \theta)^{\alpha}$ distribution in the polar angle θ with respect to the normal to the target surface at the laser focus and is uniform around the target normal in the polar angle φ. The power α of the cosine function can vary from 0 to 1 depending on the laser pulse duration, focal spot, and wavelength as well as target material composition. A value of $\alpha \sim 0.5$ is a good approximation for the picosecond laser-plasma x-ray source used in this work[1]. A collimator x-ray optic should collect the largest possible fraction[6] of the divergent plasma x-rays and efficiently redirect them in a parallel x-ray beam. Two promising approaches have been chosen to accomplish this: (1) a polycapillary x-ray optic (Fig. 8), and (2) a shaped x-ray mirror optic (Fig. 10) with enhanced reflection from a multilayer coated surface.

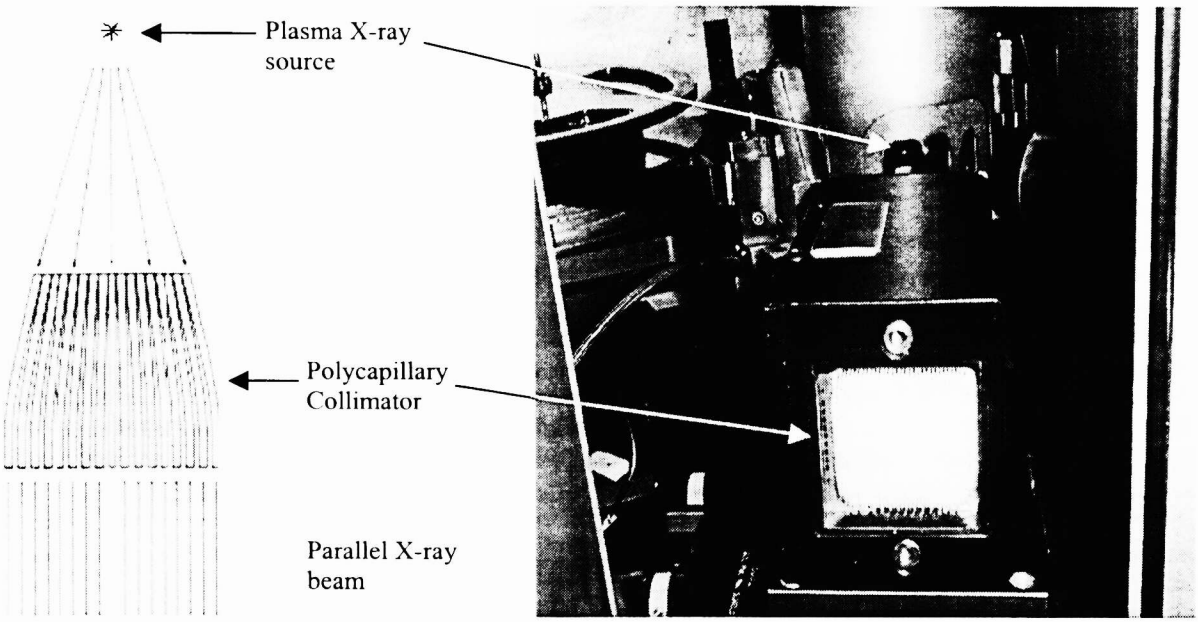

Fig. 8. Polycapillary x-ray collimator: (a) schematic operation; (b) XOS collimator mounted in the x-ray chamber. The collimator is in the central box pointing to the reader. The copper laser-plasma position is indicated by the laser spot on the copper target (inside the He flow cylinder). The parallel x-ray beam propagates from the collimator towards the reader. The laser beam propagates through the horizontal tube at the right and is incident on the target at 25^0 from the normal. The collimator collects x-rays emitted at 25^0 from the target normal (symmetric to the laser beam). A spool of copper tape target can be seen at the left of picture.

The polycapillary collimator is manufactured by X-Ray Optical Systems (XOS), Inc. It consists of 20 μm diameter hollow glass fibers which pipe the incident x-rays by multiple reflections at grazing incidence inside the fiber. By bending the

hollow glass fibers towards the plasma source (Fig. 8a) the full x-ray collection angle of 14° or a solid angle of 0.041 sr is achieved. The average transmission of the fibers is 12% over the 2 cm x 2 cm uniform x-ray beam crossection. The total collimator end-crossection is 3 cm x 3 cm. A more detailed description of the XOS collimator can be found in Refs 5 and 6 in the present SPIE volume.

Figure 8b shows the XOS collimator mounted in the x-ray chamber. The polycapillary collimator is in the central box pointing to the reader. The laser-plasma position is indicated by the light spot on the copper target (inside the He flow cylinder) and the parallel X-ray beam is propagating towards the reader. The collecting area of the collimator is placed at 8 cm from the plasma and the collimator is directed at an angle of 25° with respect to the target normal. The target contamination experiments in the previous section were carried out at the same position as the front of the collimator in order to measure any contamination on the collimator window. Several collimator characterization experiments were carried out in order to measure the collimated x-ray beam global and local divergence, uniform field size, micro-uniformity as well as the collimator gain over exposures without collimator.

Fig. 9.

(a) Intensity profile of the parallel 1 nm x-ray beam recorded on photochromic film placed 109.6 cm from the output end of the XOS polycapillary collimator

(b) Micro-densitometer trace (25 μm pixel resolution) across three horizontal sections of image (a). The trace local uniformity is within 2%. The central dip is correctable.

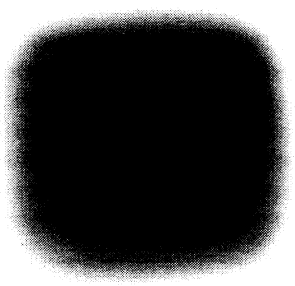

(a)

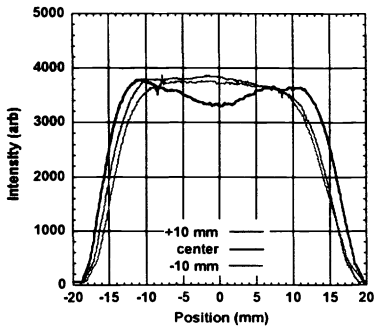

(b)

The global and local divergence measurements were obtained[5, 6] by placing a Hartman mask (containing an array of holes) in the collimated x-ray beam and analyzing the distribution of transmitted x-rays which is recorded with an x-ray CCD camera. A local divergence of less < 3 mrad and a global divergence of ~ 0.5 mrad were measured. These values meet the optimum resolution requirements for x-ray lithography of 50 -100 nm feature size. A small amount of local divergence is necessary[7, 8] in order to minimize the coherence diffraction effects or edge ringing when the 100nm features are printed from the mask onto the wafer. The field size and uniformity were measured on x-ray film and with lithographic exposures on photoresist as described in the next section. Fig. 9a shows the x-ray beam crossection recorded on photochromic film (SensorPhysics™, Model UVSC-200) placed at 109.6 cm from the output end of the XOS collimator. The 1nm x-rays are propagating through He gas from the plasma source to the x-ray film. The photochromic film has a x-ray sensitivity of 4 mJ/cm^2. It has high resolution, ≤ 1 μm since it uses a polymer as the recording medium (similar to the photoresist). No micro-nonuniformities could be seen when the film was examined under microscope. The film was scanned with a pixel resolution of 25 μm and Fig. 9b shows several microdensitometer traces across the x-ray beam profile of Fig. 9a. The collimated x-ray beam intensity profile appears to be a top hat with 2 cm x 2 cm uniform field. The local uniformity of the x-ray intensity is within the 2% requirement. The central region presents an intensity minimum. This is fully correctable and is a result of overcompensation in the collimator design. The polycapillary collimator would have an intensity maximum in the center of the field (because of the higher fiber reflectivity at smaller grazing angles) if the fibers were packed with the same density as at the field edges. In order to compensate this effect the fibers were spaced further apart at the center of the collimator field. The spacing was overcompensated and resulted in the intensity dip shown in Fig. 9. A new collimator is being designed with a more accurate compensation of this effect. X-ray film was also placed in the collimated x-ray beam at 41 cm and 51 cm from the collimator output end. While the x-ray intensity at 51.2 cm appeared similar to that at 109.6 cm, the x-ray intensity at 41.2 cm showed some field micro-nonuniformity. This is due to the fact that individual capillary x-ray beams require a minimum distance of ~50 cm to smear out and create the uniform x-ray field of Fig. 9.

The collimator gain of 10 was measured experimentally both using an e-beam x-ray source[5] and with the JMAR laser-plasma x-ray source. In the JMAR experiment, a PIN x-ray diode with a $1cm^2$ active area was placed at behind the collimator, at a distance of 58.7 cm from the plasma source. Its signal was normalized to another PIN x-ray diode looking directly to the plasma x-ray source as in Fig. 6. Both x-ray diodes are filtered with 4 μm thick Al foil. The collimator was filtered with 1.5 μm of plastic (B13) film coated with 0.8 μm of Al. The polycapillary collimator gain was measured directly from the x-ray diode signal with or without the collimator in front of it. The normalized x-ray diode signal increases 4.25 times when the collimator is inserted the diode and the plasma x-ray source. The transmission of the collimator filter is included in the above factor. The collimator gain is defined[6] is defined as the x-ray flux increase at 90cm from the plasma source when the collimator is inserted. A polycapillary collimator gain of 9.99 is found by applying the inverse square law between 90cm and the 58.7 cm distance where the measurement was made. This is good direct gain measurement since the $1cm^2$ area of the x-ray diode covers a significant fraction of the $4cm^2$ field of collimated x-ray beam.

It is instructive to evaluate the effect of such a x-ray optic on the x-ray flux delivered from the plasma source to the lithographic exposure station (Fig. 1.) The product of x-ray collection solid angle and collimator transmission is a good number to characterize the transmission function for x-rays from the point plasma source to the x-ray mask and wafer exposure station (Fig. 1.). The transfer function for the XOS collimator is $\Phi = 0.005$ sr. Using the geometry of Fig. 1 we can calculate the x-ray flux reaching the x-ray mask when the above collimator is placed in between the 100 W x-ray source and the mask/wafer exposure station. It is the product of the x-ray source emission per unit solid angle (16 W/sr) multiplied by the collimator transfer function ($\Phi = 0.005$ sr). This results in a x-ray flux of 80 mW over the 4 cm^2 x-ray beam crossection or 20 mW/cm^2. By taking into account the transmission (~50%) of the x-ray window in front of the collimator, the helium gas column from the source to the exposure cell and the x-ray mask, the x-ray flux at the photoresist on the wafer is 10 mW/cm^2 as shown in Fig. 1. The x-ray flux at the wafer from the same plasma source with no collimator is very much smaller. Because of the divergence of the x-rays emitted by the plasma source the mask/wafer exposure station would need to be placed at 90 cm from the source. Therefore the solid angle subtended by 1 cm^2 at the resist would be 1.2×10^{-4} sr and the x-ray flux at the wafer from a 100 W x-ray source would be $100 \text{ W} \div 2\pi \times 1.2 \times 10^{-4}$ sr x 50% = 1 mW /cm^2. This shows that the XOS collimator increases the x-ray flux to the wafer ten fold or the collimator has a "gain" of 10. Apart from the gain, the parallelism of the collimator x-ray beam is essential for proximity lithography of feature sizes of 100 nm and smaller.

The second type of collimator we are developing for the plasma x-ray source is the shaped x-ray mirror collimator, shown in Fig. 10, which designed and manufactured at the Lawrence Livermore National Laboratory. The principle of x-ray collection and beam collimation is shown in Fig. 10a and consists of bending the diverging x-ray beams with one reflection on the inner surface of the collimator. The collimator is placed 5 cm from the plasma x-ray source and has a collection solid angle of 0.048 sr. The collimator is 10 cm long and has an input diameter of 15 mm and output diameter of 25 mm. The x-ray beam emerging from the collimator has the shape of an annulus 10 mm wide with outer diameter of 25 mm and inner diameter of 15 mm. This annular beam is then scanned in order to achieve uniform illumination on the mask and wafer. This collimator is designed to illuminate a large exposure field of 25mm x 36 mm. The scanning technique allows even larger exposure fields if necessary. The reflectivity of the collimator is ~10% after spectral averaging over the Cu L-shell x-ray emission spectrum and range of angles of incidence. The x-ray source-to-wafer transfer function of the LLNL collimator is similar to the XOS collimator. The LLNL collimator x-ray mirror surface, which is presently metallic, will be replaced with a multilayer coating with enhanced collection (grazing) angle and reflectivity. The collimator gain will then increase from the present 2 times to 12 times due to the larger collection angle and reflectivity. The present gain measurements were made by taking the ratio of the x-ray intensity between the bright rings of collimated x-rays and the center of the collimator directly illuminated by plasma source. The x-rays were recorded with a x-ray CCD camera. The collimator could be manufactured in multiples by replication from a mandrel. Fig. 10b (center) shows the highly polished mandrel manufactured by Baker Consulting, CA. On either side are the two replica collimators, which were used in our tests. This method of fabrication represents a breakthrough in x-ray optics manufacturing. It eliminates the difficulty of having to polish the optic on the inside since the mandrel is polished on the outside. It also reduces the cost of each optic since from a single mandrel one can obtain several replicas. A more detailed description of the LLNL collimator can be found in Ref. 6 in the present SPIE volume.

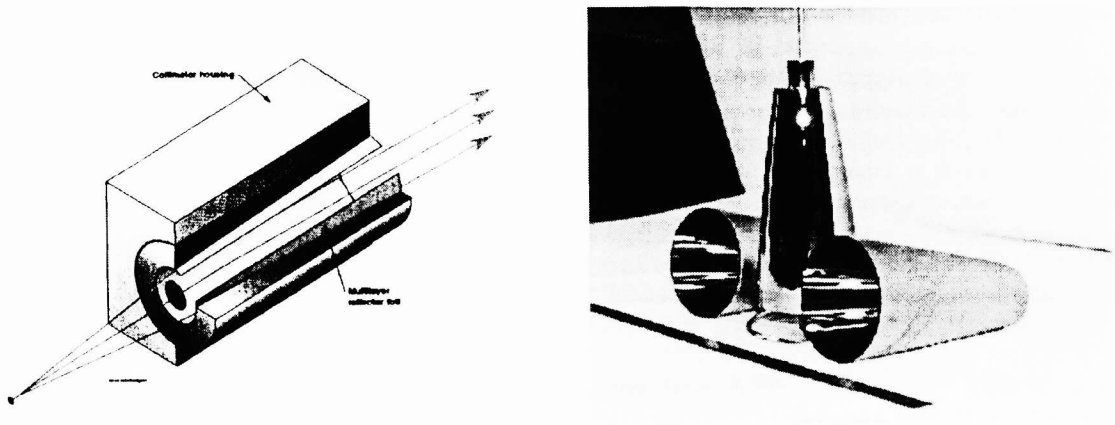

(a) (b)

Fig. 10. Shaped x-ray mirror LLNL collimator. (a) Schematic of x-ray collection from the plasma source and generation of a parallel annular x-ray beam. (b) Two identical x-ray collimators replicated from one mandrel.

The LLNL collimator is characterized in the same way as the XOS collimator discussed above. The global divergence is ~1 mrad, the local divergence ~0.4 mrad. The gain of the metal collimator is 2. This is only a test bed for the resonant reflector collimator, which will have a gain of 12 at 90 cm from the plasma source. The field uniformity measurements show a number of intensity rings instead of a uniformly illuminated annulus. This is due to a small figure error in the manufacture of the mandrel. This error corresponds to a sinusoid with an amplitude of 1 μm over a mandrel length of 3 cm. The figure error will be improved due to the increased resolution (0.1μm) in the metrology of the mandrel surface. Of great importance is the result, which show that the collimated x-ray beams from the two sister replicas (Fig. 10b.) are identical. It confirms the concept that several collimators can be successfully replicated from one mandrel.

Both collimators show potential for generating a parallel x-ray beam from the plasma x-ray source. The LLNL collimator with resonant reflection coating will have higher gain than the XOS collimator. On the other hand the XOS collimator produces a full field x-ray beam whereas the annular x-ray beam of the LLNL collimator needs to be scanned across the lithographic exposure field.

6. WAFER EXPOSURE WITH COLLIMATED X-RAYS

High-resolution lithography is performed for the first time with parallel X-rays obtained by collimated 1nm radiation from the laser-plasma source in the exposure geometry shown in Fig. 1. The Britelight™ laser beam is converted from IR to green. The laser repetition rate is 300 Hz. The x-ray chamber, collimator and mask wafer exposure cell are kept in helium gas at 100 torr pressure. The x-ray exposure cell (mask and wafer) is placed at 54 cm distance from the output end of the XOS collimator. An IBM high-resolution SiC-Ta x-ray mask with 160 nm minimum feature size is used. The mask-to-wafer gap is maintained by plastic shims 12.5 μm thick. The wafer is coated with chemically amplified SU8 resist, 0.5 μm thick. The x-ray sensitivity of SU8 resist is 60 mJ/cm^2. A thin plastic (B-13 polyester 1.5 μm thick coated with 0.8 μm Al) filter is placed in front of the collimator. Fig. 11a shows SEM images of the exposed photoresist with a parallel x-ray beam from the XOS collimator and Fig. 11b from the LLNL collimator. The mask features are printed accurately on the resist. The smallest mask feature in the exposure field is 200 nm. The slight waviness is due to the development process of the chemically amplified resist. X-ray exposure duration is 5 min to 15 min for the LLNL and XOS collimator, respectively. (The LLNL collimator was not scanned, and has much higher flux in the annulus illumination than the uniform case when scanned.) With a more sensitive resist (15 mJ/cm^2) and ten times more x-ray power of the PXS system described in the next section, the exposure time of a full field will be reduced to a few seconds.

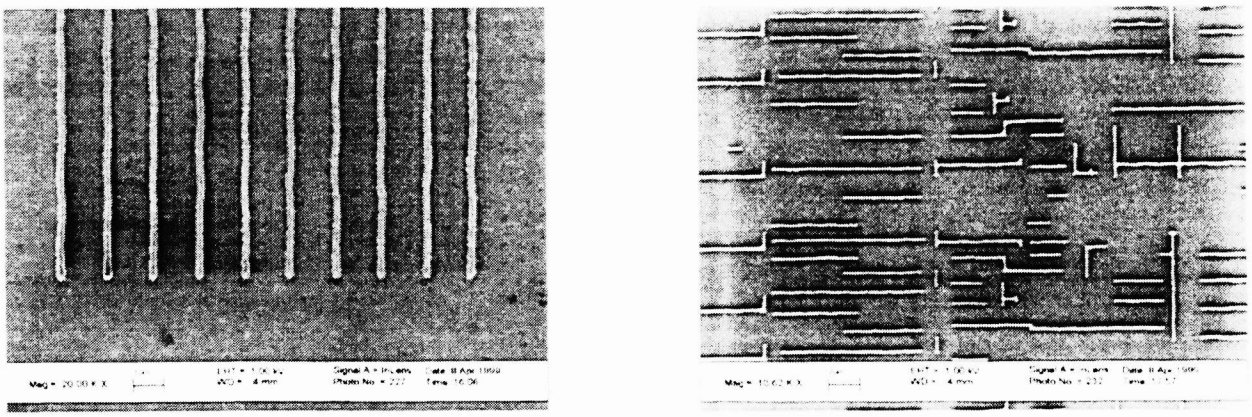

(a) (b)

Fig. 11. High resolution lithography with collimated 1nm x-rays from the laser-plasma source. The SEM images of the exposed photoresist replicate the features on the x-ray mask which have linewidth of 200 nm. (a) X-ray exposure using the XOS collimator. (b) X-ray exposure using the LLNL collimator. The slight line waviness is due to a slight temperature non-uniformity in the development process of the chemically amplified x-ray photo-resist.

7. SCALING IN X-RAY POWER

According to the concept shown in Fig 2, JMAR is constructing a multi-beam system that is capable of much higher x-ray power. Figure 12a shows a brassboard system having one master oscillator, a pre-amplifier stage, and 8 independent amplifiers to produce 8 laser beams that are simultaneously input to the x-ray target chamber. Between the laser amplifiers and the target chamber is a beam forming section that allows frequency doubling, beam combining to superpose two beams at a time, and beam expansion. The four sets of two beams are then directed into four symmetrically located lens tubes on the front face of the target chamber. The eight beams are focussed onto a copper tape in a controlled cluster pattern approximately 200 microns in diameter, and create simultaneous, independently radiating x-ray point sources. The eight or more micro x-ray sources can be distributed in any other desired configuration. Each beam is designed to produce approximately 3 watts (average) of 1 nm x-rays, and it is expected that all eight beams would produce at least 24 watts of 1 nm x-ray total power. The lasers in this system are presently beginning operation.

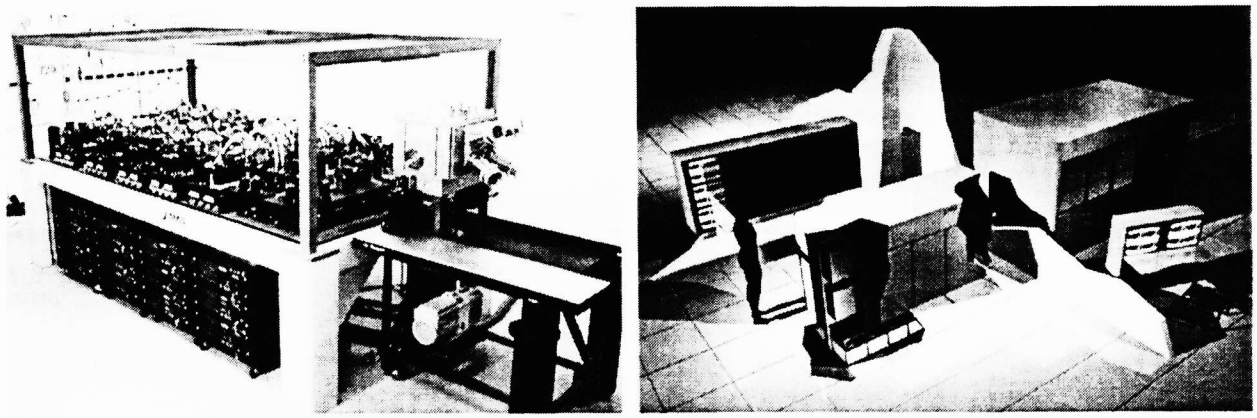

Fig. 12. High x-ray power, multiple laser-beam PXS system. (a) Eight laser beam brass-board system to develop multi-beam concept and evaluate details of the approach. The x-ray chamber is shown at the right. Its four arms focus four pairs of laser beams on the copper tape target. The x-ray chamber is filled with He gas at atmospheric pressure. (b) A concept of how this system can be packaged as a next generation x-ray lithography tool.

Figure 12b shows a concept of how this system can be repackaged for a semiconductor lithography application. The unit in the foreground contains all the laser components for a 16 beam system mounted on two sides of a vertically oriented platform. The beam forming section and the x-ray chamber are also included at the end of this unit. To the right is an environmental chamber containing the lithography stepper where wafers are exposed through a x-ray mask. The laser system electronics are located remotely in the unit to the left, are controlled by the user console shown at right. Water cooling systems for the lasers is located under the floor. With 16 laser modules, each having 200 Watts average IR power, this x-ray lithography system is projected to be capable of a throughput of ~20 each 300 mm wafers per hour to meet NGL needs.

8. CONCLUSIONS

The work reported in this paper demonstrates for the first time a number of key elements required for commercial implementation of soft x-ray proximity printing for the Next Generation Lithography technology. A compact x-ray source is generated by a compact diode pumped laser system. A single laser amplifier module generates a copper plasma which radiates an x-ray power of 2.8 Watts at 1nm wavelength. The laser-plasma x-ray source is operated with negligible target material contamination of the exposure station. A uniform parallel x-ray beam is generated using efficient x-ray collimators. The parallel x-ray beam from the compact x-ray source prints 200nm structures in photoresist, accurately replicating the x-ray mask features. The x-ray source is being scaled up in a compact, parallel laser amplifier system. This lithographic tool is expected to have a throughput of over 20 Wafer Levels per Hour for 300 mm diameter wafers with printed features of 130nm and next generations of 100 nm, 70 nm and beyond.

ACKNOWLEDGEMENTS

We thank Ms M.A. Zaitz of IBM Hopewell Junction facility for the wafer contamination analysis, J. Honig of LLNL for diode laser pumping simulations and M. Peckerar of NRL for providing the x-ray masks. We also thank J. Morris, B. Roberts, P. Hark, D. Saffold, C. Kelsey, T. LaCour, R. Healy, R. Taylor, G. Saldana, C. Cardinez, E. Waltz, J. Mix of JMAR Technologies, Inc., for their contribution to the construction of the eight laser beam scaled up Picosecond X-Ray Source.

This work was performed for the US Government's Defense Advanced Research Agency, Advanced Lithography Program, Dr David O. Patterson, under contract with Army Research Laboratory, R.B. Reams, No. DAAL01-98-C-0042.

REFERENCES

1. I.C.E. Turcu, J.B. Dance, "X-rays from laser plasmas: generation and applications", J. Wiley & Sons, Chichester, 1999.
2. H. Rieger, S. Campeau, "High brightness and power Nd:YAG laser", in "Advanced solid state lasers", M.M. Feyer, H. Injeyan, U. Keller eds., **OSA TOPS** Vol. **26**, 49-53, Optical Society of America, 1999.
3. H. Shields, at al., "High power excimer laser-generated plasma source for x-ray micro-lithography", in Proc. Soc. Photo-Opt. Instrum. Eng., "Applications of laser plasma radiation II" M.C. Richardson, G.A. Kyrala, Eds., **SPIE 2523**, 122-8 (1995).
4. M. Chacker, et al., "Laser plasma x-ray sources for micro-lithography", J. Appl. Phys., **63**, 892-8 (1988).
5. Z Chen et al., "Polycapillary collimator for plasma-source x-ray lithography", in Proc. Soc. Photo-Opt. Instrum. Eng., "EUV, X-Ray, and Neutron optics and sources", **SPIE 3767,** in print 1999.
6. S.M. Lane et al., "Review of x-ray collimators for x-ray proximity lithography", in Proc. Soc. Photo-Opt. Instrum. Eng., "EUV, X-Ray, and Neutron optics and sources", **SPIE 3767,** in print 1999.
7. H.I. Smith, "X-ray lithography: will it make it in manufacturing?", in Short Course Notes **SC02**, **SPIE** Ann. Int. Symp. Microlithography, February 1995.
8. F. Cerrina, "X-ray lithography", in Short Course Notes **SC02**, **SPIE** 23rd Ann. Int. Symp. Microlithography, February 1998.